

# INVESTIGAREA FORMĂRII FAZELOR ȘI A PROPRIETĂȚILOR ELECTRICE A PZT DOPAT CU Fe PENTRU O APLICAȚIE AVANSATĂ

## INVESTIGATION OF PHASE FORMATION AND ELECTRICAL PROPERTIES OF Fe-DOPED PZT FOR ADVANCED APPLICATION

ALINA IULIA DUMITRU<sup>1,2</sup>, GEORGETA VELCIU<sup>1\*</sup>, DELIA PĂTROIU<sup>1</sup>, JANA PINTEA<sup>1</sup>, VIRGIL MARINESCU<sup>1</sup>, TUDOR-GABRIEL DUMITRU<sup>3</sup>, ILDIKO PETER<sup>4\*</sup>

<sup>1</sup>National Institute for Research & Development in Electrical Engineering ICPE-CA, 313 Splaiul Unirii, 030138, Bucharest, Romania

<sup>2</sup>University of Valahia, Str. Aleea Sinaia, nr. 13, 130004 Târgoviște, Romania

<sup>3</sup>University of Bucharest, Faculty of Physics, Str. Atomistilor, Măgurele, Romania

<sup>4</sup>University of Medicine, Pharmacy, Science and Technology „George Emil Palade”

Faculty of Engineering and Information Technology Str. Nicolae Iorga nr. 1, Târgu-Mureș, 540139, Romania

*In this paper, some compositions described by the general formula  $Pb(Zr_{\lambda}Ti_{1-\lambda})_{1-3x/4}Fe_xO_3$  have been considered and investigated. The compositions selected have been obtained by solid state reaction, where  $x=0.01$  and  $\lambda$  corresponds to 0.42, 0.52 and 0.58. The samples have been thermally treated in the range of 1100°C -1250°C and holded for 2 hours at the maximum temperature.*

*The influence of the sintering temperature on the microstructure and on the electrical properties of  $Fe^{3+}$  doped  $Pb(Zr_{\lambda}Ti_{1-\lambda})O_3$  system has been investigated. The crystallographic phase and microstructure of the sintered compositions has been studied in detail using X-ray diffraction analysis (XRD) and Scanning Electron Microscopy (SEM). The experimental results obtained by XRD revealed that all the sintered samples have a perovskite structure. In order to correlate the behavior of the sintered materials to their microscopic structure, the domain structures have been defined by SEM. The dielectric properties, as dielectric permittivity ( $\epsilon_r$ ) and dielectric loss ( $\tan\delta$ ) have been measured. The hysteresis loops at room temperature of all un-poled sintered compositions reveal a similar behaviour with “hard” PZT ceramics. The piezoelectric properties like electromechanical coupling factors ( $k_p$  and  $k_t$ ) and the anisotropy ( $k_t/k_p$ ) have been investigated after polarization. The results obtained from such investigations pointed out that some sintered compositions can be successfully proposed as good candidate for targets, materials to be deposited, employed for different applications as ceramic coatings in some deposition technology.*

*În această lucrare, au fost luate în considerare și investigate câteva compoziții descrise de formula generală  $Pb(Zr_{\lambda}Ti_{1-\lambda})_{1-3x/4}Fe_xO_3$ . Compozițiile selectate au fost obținute prin reacții în stare solidă, unde  $x = 0,01$  și  $\lambda$  corespunde cu 0,42, 0,52 și 0,58. Probele au fost tratate termic în intervalul 1100°C -1250°C și ținute timp de 2 ore la temperatura maximă.*

*S-a investigat influența temperaturii de sinterizare asupra microstructurii și asupra proprietăților electrice ale sistemului  $Pb(Zr_{\lambda}Ti_{1-\lambda})O_3$  dopat cu  $Fe^{3+}$ . Faza cristalografică și microstructura compozițiilor sinterizate au fost studiate în detaliu utilizând analiza de difracției cu raze X (DRX) și microscopia electronică de scanare (MES). Rezultatele experimentale obținute de DRX au dezvăluit că toate probele sinterizate au o structură de perovskit. Pentru a corela comportamentul materialelor sinterizate cu structura lor microscopică, structura domeniilor au fost definite de analizele MES. S-au măsurat proprietățile dielectrice, precum permitivitatea dielectrică ( $\epsilon_r$ ) și pierderea dielectrică ( $\tan\delta$ ). Buclele de histeresis la temperatura camerei ale tuturor compozițiilor sinterizate nepolarizate demonstrează un comportament similar cu ceramica PZT „dură”. Proprietățile piezoelectrice cum ar fi factorii de cuplare electromecanici ( $k_p$  și  $k_t$ ) și anizotropia ( $k_t/k_p$ ) au fost investigate după polarizare. Rezultatele obținute în urma unor astfel de investigații au arătat că unele compoziții sinterizate pot fi propuse cu succes ca fiind un bun candidat pentru ținte, materiale pentru depuneri în unele tehnologii de depunere, utilizate pentru diferite aplicații precum acoperirile ceramice.*

**Keywords:** doped PZT, dielectric properties, piezoelectric properties, ferroelectric properties

### 1. Introduction

Lead zirconate titanate (noted PZT or  $Pb(Zr_{\lambda}Ti_{1-\lambda})O_3$ ) is very attractive material for its properties designing. Wide range of electrical/ piezoelectrical/ ferroelectrical properties can be obtained varying the Zr/Ti ratio in the  $PbTiO_3$ - $PbZrO_3$  diagram, particularly in a so-called morphotropic phase boundary (MPB) region [1]. PZT materials are almost always used with one or more dopants to improve and optimize their basic properties for specific applications [1,2]. Acceptor dopants, such as  $Fe^{3+}$  replacing ( $Zr^{4+}$ ,  $Ti^{4+}$ ), are compensated by oxygen vacancies and usually have a limited solubility in the lattice. Domains

reorientation are limited and compositions with acceptor dopants are more difficult to pole and usually are characterized by poorly developed hysteresis loops, low dielectric losses, lower dielectric constant, low piezoelectric properties, higher ageing rate. These materials are called “hard” PZT [1].

From the beginning, the  $PbTiO_3$ - $PbZrO_3$  diagram has been in many researchers' attention. From on hand, Isupov [3,4] have reported that the tetragonal and rhombohedral phases are stable in a region at the morphotropic boundary. On the other hand, Ari-Gur et al. [5] have indicated that the value of x for the tetragonal phase is lower than that of the

\* Autor correspondent/Corresponding author,

E-mail: [georgeta.velciu@icpe-ca.ro](mailto:georgeta.velciu@icpe-ca.ro), [ildiko.peter@umfst.ro](mailto:ildiko.peter@umfst.ro)

rhombohedral phase. Such region is an area where these two phases coexist. M. Morozov [6] have studied the well-known “soft” materials PZT (PZT doped with Nb) and “hard” PZT (PZT doped with Fe) belonging to the three regions of the  $\text{PbTiO}_3$ - $\text{PbZrO}_3$  diagram, in order to determine the key principles which are necessary for a physical model of hysteresis and nonlinearity. In the  $\text{PbTiO}_3$ - $\text{PbZrO}_3$  diagram there are four compositional regions for the solid solutions described by the general formula  $\text{Pb}(\text{Zr}_\lambda\text{Ti}_{1-\lambda})\text{O}_3$  [1,6]. Depending on the values of  $\lambda$ , the solid solutions of the  $\text{Pb}(\text{Zr}_\lambda\text{Ti}_{1-\lambda})\text{O}_3$  compositions are located in one of the four regions. These regions are characterized by specific properties and applications according also to [7].

In the first region  $0 < 1-\lambda < 0.1$ , the obtained materials are characterized by two phases under normal conditions (ferroelectric phase and antiferroelectric phase) [6]. The transition from the antiferroelectric phase to the ferroelectric phase under the action of the external electric field can be exploited in shape memory applications, while the transition from the ferroelectric phase to the antiferroelectric phase under the external action of a mechanical force and the electric field is useful in obtaining elements with high electron emissions [6,8].

The second region with  $0.1 < 1-\lambda < 0.4$  is characterized by two rhombohedral phases [6]. The materials belonging to this region are described by a high pyroelectric effect and used in pyroelectric detectors. For doped compositions located in this second region, the metastable polarization state is decisive, this condition is typical of relaxor materials. These materials are used in the development of devices with surface acoustic waves and electromechanical transducers [6,9].

The most studied region is the third region and it includes the area called the morphotropic phase limit (MPB)  $0.4 < 1-\lambda < 0.6$  [6]. This limit separates the rhombohedral area from the tetragonal area. In this region the properties are strongly influenced by the value of  $\lambda$ . The compositions for  $\text{Zr}/\text{Ti} = 52/48$  are characterized by a single phase tetragonal perovskite type [3,4,10,11]. Compositions in the vicinity of MPB are characterized by maximum values for most properties. These values are used in some applications of these materials [12,13].

The fourth region with  $0.6 < 1-\lambda < 1.0$  is the region of compositions with high anisotropy [6]. The materials in this area show high anisotropy of the piezoelectric coefficients  $d_{31}$  and  $d_{33}$  and of the electromechanical coupling factors  $k_p$  and  $k_t$  [14]. The compositions are characterized by spontaneous deformations and high coercive field values. Materials belonging to this area are used in applications such as filters and frequency stabilizers.

In the present paper, new PZT based compositions doped with  $\text{Fe}^{3+}$ , being in three

regions of the  $\text{PbTiO}_3$ - $\text{PbZrO}_3$  diagram, where  $\text{Fe}^{3+}$  as an acceptor ion may replace  $\text{Ti}^{4+}$  site have been considered and investigated. The main objective of the research is related to study the above mentioned compositions focalizing on the determination of the structural and electrical properties of the materials synthesized with  $\text{Fe}^{3+}$  substitution on the B site of  $\text{Pb}(\text{Zr}_\lambda\text{Ti}_{1-\lambda})\text{O}_3$  system in order to obtain innovative materials. These new materials with the general formula of  $\text{Pb}(\text{Zr}_\lambda\text{Ti}_{1-\lambda})_{1-3x/4}\text{Fe}_x\text{O}_3$  will be efficiently used in the development of targets for the deposition technology.

## 2. Experiments

New ferroelectric samples with a general formula  $\text{Pb}(\text{Zr}_\lambda\text{Ti}_{1-\lambda})_{1-3x/4}\text{Fe}_x\text{O}_3$  with  $x = 0.01$  and  $\lambda$  having the values 0.42, 0.52 and 0.58 have been synthesized by solid state reaction using high temperature. The compositions have been labelled PZTF-42 (with  $\text{Zr}/\text{Ti}$  ratio 42/58), PZTF-52 (with  $\text{Zr}/\text{Ti}$  ratio 52/48) and PZTF-58 (with  $\text{Zr}/\text{Ti}$  ratio 58/42).

All the compositions have been obtained using high purity oxides ( $\geq 99\%$ ) like  $\text{PbO}$  (from Merck),  $\text{TiO}_2$  (from Aldrich),  $\text{ZrO}_2$  (from Merck), and  $\text{Fe}_2\text{O}_3$  (from Merck). The oxides powders were ball-milled wet for 10 h, the ratio balls:mixture:ethanol was of 1:1:1 and calcined at  $870^\circ\text{C}$  for 4 h. The calcined powders were ball-milled again in ethanol for 10 h, dried, mixed with binder 5 wt% polyvinyl alcohol (PVA) solution and pressed uniaxial at 70 MPa in discs shape with 10 mm diameter. Discs have been thermal treated in air for 2 hours at  $1100^\circ\text{C}$  -  $1250^\circ\text{C}$  in locked alumina crucible and a lead rich atmosphere ( $\text{PbZrO}_3$ ) with controlled cooling in furnace.

Experimental density of all sintered discs were measured by Archimedes method. The phases formation in the sintered discs were studied with X-ray diffractometer (XRD) using BRUKER AXS D8 Advance with  $\text{CuK}\alpha$  radiation with a 1D LynxEye detector and Ni filter at room temperature in Bragg-Brentano geometry, at a scan speed of 1s/step and incremental  $2\theta$  angle of  $0.04^\circ$ .

Microstructure and grain size were studied by scanning electron microscopy (SEM) using FESEM-FIB Workstation Auriga produced by Carl Zeiss, Germany. Before using for electrical measurements all the sintered discs have been electrode on both sides by silver paste and fired at  $650^\circ\text{C}$  for 30 min. Relative dielectric constant ( $\epsilon_r$ ) and loss tangent ( $\tan \delta$ ) were measured at room temperature at 1 kHz using LCR meter HM 8018. Ferroelectric hysteresis behaviour (P-E) of the unpoled discs were measured using the TF analyser 2000. To determine the piezoelectric properties, the sintered discs were poled in a silicon oil bath at  $100^\circ\text{C}$  for 30 minutes in a DC field of 3.5 kV/mm. Piezoelectric properties were determined after 24 h from polarization using impedance analyser 4294A

Table 1

Behaviour of the samples after thermal treatment for new compositions/Comportamentul probelor după tratamentul termic pentru compoziții noi

Temperature [°C]	Samples	Experimental density [g/cm <sup>3</sup> ]	Relative density [%]	Region
1100	PZTF-42	7.43	95.26	T
	PZTF-52	7.42	95.13	MPB
	PZTF-58	7.41	95.00	RH
1150	PZTF-42	7.47	95.77	T
	PZTF-52	7.48	95.90	MPB
	PZTF-58	7.47	95.77	RH
1200	PZTF-42	7.56	96.23	T
	PZTF-52	7.68	98.46	MPB
	PZTF-58	7.49	96.02	RH
1250	PZTF-42	7.65	98.08	T
	PZTF-52	7.72	98.97	MPB
	PZTF-58	7.57	97.05	RH

by the resonance ( $f_r$ ) and antiresonance ( $f_a$ ) frequency method [15].

### 3. Results and discussions

#### 3.1. Behaviour of the samples at thermal treatment

The addition of donor or/and acceptor dopants (like Fe<sup>3+</sup>, Ni<sup>2+</sup>, Mn<sup>2+</sup>, Sb<sup>3+</sup>, Nb<sup>5+</sup>, etc.) in Pb(Zr<sub>λ</sub>Ti<sub>1-λ</sub>)O<sub>3</sub> system influences the microstructure and electrical properties of the compositions [16-19].

The final properties, obtained after the thermal treatment, depend on the value of the Zr/Ti ratio. By adding acceptor ions such as Fe<sup>3+</sup> (for B site) in the Pb(Zr<sub>λ</sub>Ti<sub>1-λ</sub>)O<sub>3</sub> system (ABO<sub>3</sub>), "hard" materials have been developed, according also to [20]. The introduction of Fe<sup>3+</sup> ions as a dopant leads to oxygen vacancies. In order to increase the accuracy of the measurements, heavy samples have been used (>3 g). In this paper the authors assume that the theoretical density of all studied PZT compositions is 7.8 g/cm<sup>3</sup> similar to some studies reported in the scientific literature [21]. The results indicate that the relative density of all sintered sample is situated above 95% at least (Table 1). The increase of the thermal treatment led to the increase of the density for all the studied compositions. The density values, obtained for the three compositions, are very similar, which indicates a good densification of the materials regardless of the chosen region.

For thermal treatments with a temperature higher than 1100°C the highest density value is obtained for the composition PZTF-52 which is located in the morphotropic phase limit (MPB).

The relative density increases as the temperature increases (from 1100°C to 1250°C), reaching up to 98% of the theoretical density for the PZTF-52 sample.

#### 3.2. Structural analysis

Since Fe<sup>3+</sup> is known as a hard dopant, it is expected to replace Ti<sup>4+</sup> or Zr<sup>4+</sup> in B positions of the perovskite structure (ABO<sub>3</sub>), therefore giving rise to

a lattice distortion and appearance of structural vacation. Figures 1-4 show the experimental XRD patterns for each sintering temperature.

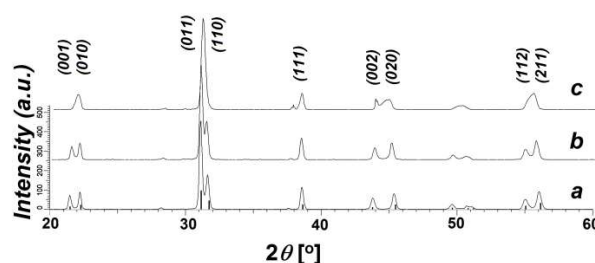


Fig. 1 - XRD patterns for (a) PZTF-42, (b) PZTF-52, (c) PZTF-58 at 1100°C/ Diagramele de raze X la 1100°C pentru (a) PZTF-42, (b) PZTF-52, (c) PZTF-58.

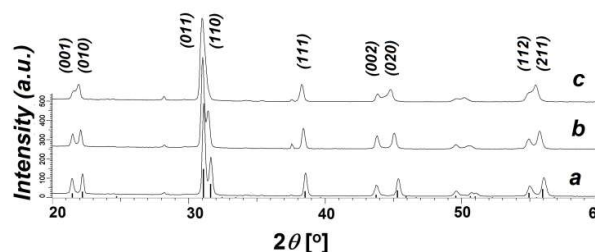


Fig. 2 - XRD patterns for (a) PZTF-42, (b) PZTF-52, (c) PZTF-58 at 1150°C/ Diagramele de raze X la 1150°C pentru (a) PZTF-42, (b) PZTF-52, (c) PZTF-58.

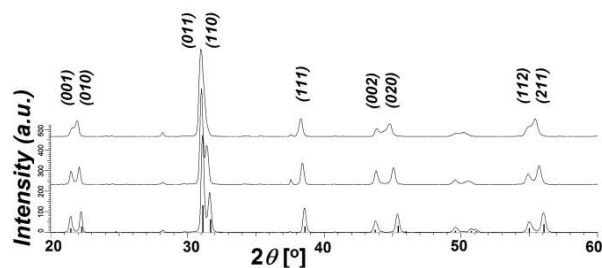


Fig. 3 - XRD patterns for (a) PZTF-42, (b) PZTF-52, (c) PZTF-58 at 1200°C/ Diagramele de raze X la 1200°C pentru (a) PZTF-42, (b) PZTF-52, (c) PZTF-58.

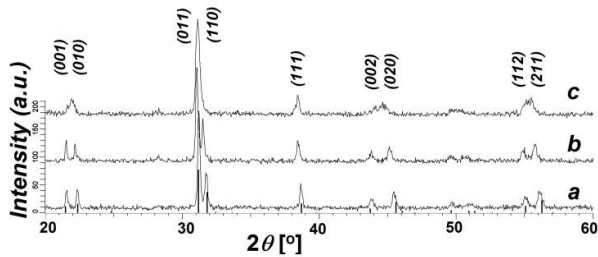


Fig. 4 - XRD patterns for (a) PZTF-42, (b) PZTF-52, (c) PZTF-58 at 1250°C/ *Diagramele de raze X pentru (a) PZTF-42, (b) PZTF-52, (c) PZTF-58 la 1250°C.*

All XRD patterns show the main tetragonal crystalline phase indicating the perovskite solid solution phase formation (ICDD PDF2 # 01-070-4060). For PZTF-52 and PZTF-58 at lower sintering temperatures (1100°C-1200°C), splitting of (111) peak, at angular position of  $2\theta \sim 38^\circ$ , reveals an additional rhombohedral structure due to the  $\text{Fe}^{3+}$  dopant which acts as structural defect influencing the transformation of the rhombohedral cell into a tetragonal one. At 1250°C the unique phase detected is the tetragonal one for all the compositions due to the increase of the dopant ( $\text{Fe}^{3+}$ ) thermal mobility.

The displacements of the specific lines of the perovskite structure ( $\text{ABO}_3$ ) can be attributed to the distortion of the crystalline structure due to the presence of the dopant ( $\text{Fe}^{3+}$ ) into some specific position (B positions), which seems to be more relevant in such structures.

### 3.3. Electron microscopy studies

As from the Figs. 5-8, the microstructure of all sintered compositions is relatively homogeneous and fine grained, with an average grain size depending on the Zr/Ti ratio and on the sintering temperature.

Fig.5 and Fig.7 show the electron microscopy images of the thermally treated (at 1100°C and 1200°C) sample which have been etched with a HCl and HF solution.

SEM images at 50.00 kX magnifications for the compositions thermally treated at 1100°C show a microstructure with small pores and uniformly distributed small grains mostly located at the limit of the growth grains. The average small grains size of the all samples was found to be 0.27  $\mu\text{m}$  and 0.41  $\mu\text{m}$ . Also, the average for the large grains was 1.05  $\mu\text{m}$  – 1.92  $\mu\text{m}$  for samples thermally treated at 1100°C.

At 1150°C (Figs. 6 (a-c)) the SEM images (50.00 kX magnification) are similar to the previous ones and show a morphology with the similar average small granules (0.125  $\mu\text{m}$ ) mostly positioned at the limit of the large grains with average dimensions of 1.75  $\mu\text{m}$ . It was found that the grains of different sizes are uniformly distributed in all the sintered compositions. Additionally, porosity of the samples was observed.

At 1200°C (Fig.7 - 20.00kX magnification) and 1250°C (Fig.8 - 20.00kX magnification) all compositions become much denser. It comes out

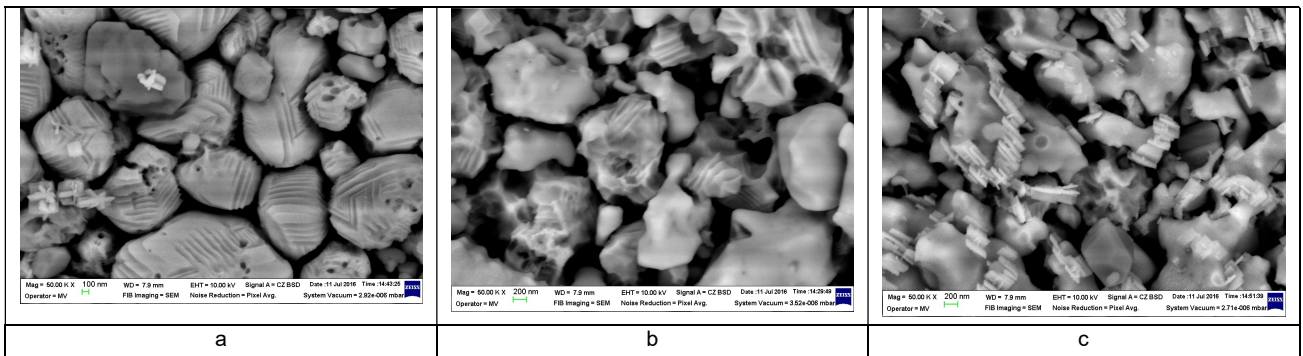


Fig. 5 - SEM images of the compositions thermally treated for 2 h at 1100°C (a) PZTF-42, (b) PZTF-52 and (c) PZTF-58/ *Imaginile SEM ale compozițiilor (a) PZTF-42, (b) PZTF-52 și (c) PZTF-58 tratate termic la 1100°C pentru 2 h.*

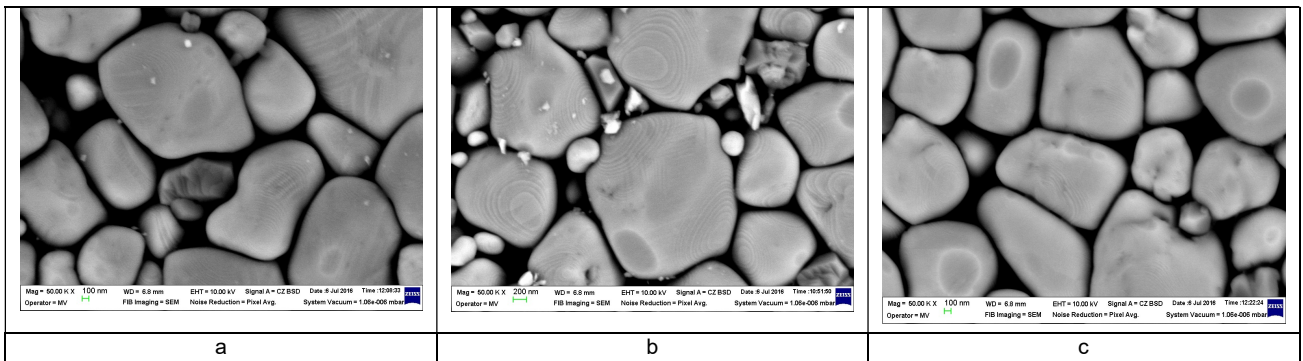
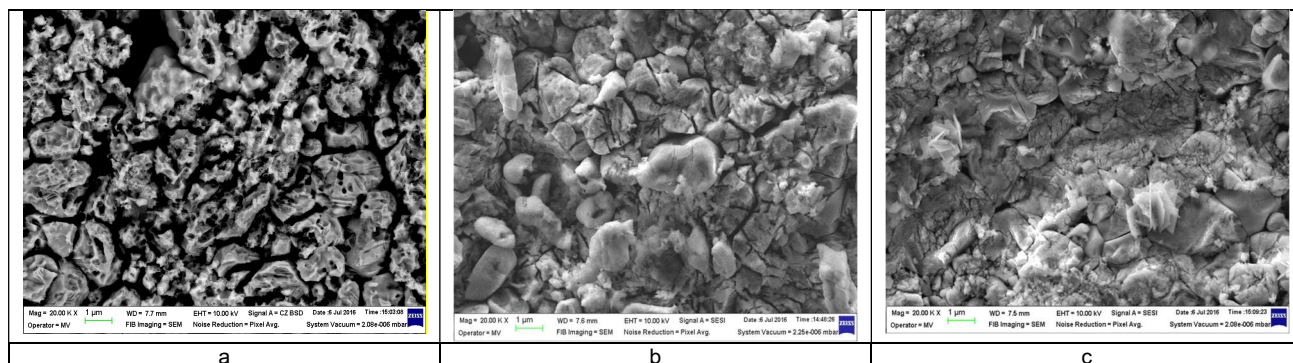
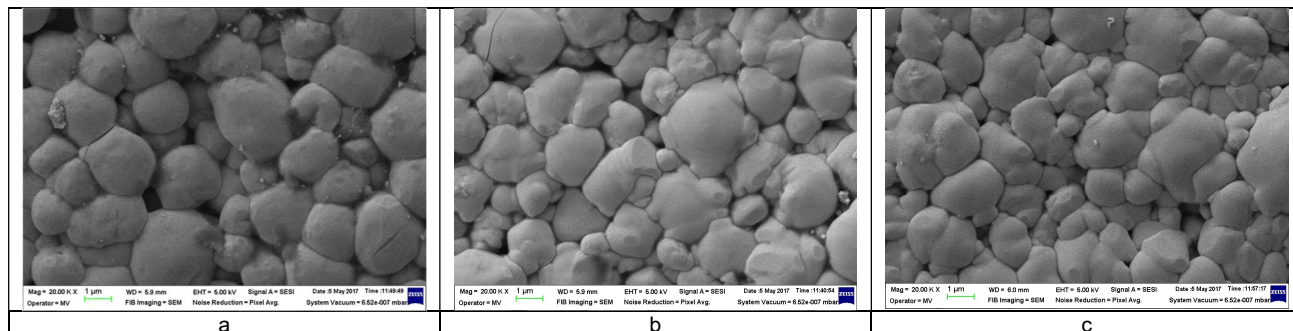


Fig. 6 - SEM images of the compositions thermally treated for 2 h at 1150°C (a) PZTF-42, (b) PZTF-52 and (c) PZTF-58/ *Imaginile SEM ale compozițiilor (a) PZTF-42, (b) PZTF-52 and (c) PZTF-58 tratate termic la 1150°C pentru 2 h.*



**Fig. 7** - SEM images of the compositions thermally treated for 2 h at 1200°C (a) PZTF-42, (b) PZTF-52 and (c) PZTF-58/ *Imaginile SEM ale compozițiilor (a) PZTF-42, (b) PZTF-52 și (c) PZTF-58 tratate termic la 1200°C pentru 2 h.*



**Fig. 8** - SEM images of the compositions thermally treated for 2 h at 1250°C (a) PZTF-42, (b) PZTF-52 and (c) PZTF-58/ *Imaginile SEM ale compozițiilor (a) PZTF-42, (b) PZTF-52 și (c) PZTF-58 tratate termic la 1250°C pentru 2 h.*

that the sintering temperature and the Zr/Ti ratio have a decisive role in obtaining the shape and the size of the grains. Replacement of  $Zr^{4+}$  with  $Fe^{3+}$  leads to an increase in the grains size of the compositions which has also been reported by other researchers [22].

In all cases, the MPB composition (PZTF-52) has a denser microstructure than the other two compositions located in the tetragonal region (PZTF-42) and rhombohedral region (PZTF-58).

The decrease of the crystallites and the grain sizes could be due to the size mismatch of  $Fe^{3+}$  (0.64Å) and  $Zr^{4+}$  (0.80Å) ions, which creates a tension in the lattice. Fe-doping plays an important role in the control of grain growth, possibly due to the oxygen vacancy formation, which could stop the grain boundary migration.

### 3.4. Ferroelectric characteristics

In Figs. 9-12 the ferroelectric hysteresis loops of all un-poled compositions which have been thermally treated for 2 hours at 1100°C, 1150°C, 1200°C and 1250°C at room temperature have been reported. It can be observed that all compositions shows hysteresis loops which are similar to the hysteresis loops of the hard materials. The obtained results are in a good agreement with some data reported by other researchers [23,24]. Domains reorientation are limited, and, all compositions are characterized by poorly developed hysteresis loops. The motion of the domains walls influences the direction in which the electrical coercivity and remanent polarization are changing [25]. The

presence of the domain walls is a result of multidomain structure of many ferroelectric crystals.

The motion of the domains walls is influenced by the grain size of the compositions and the type of vacancy defects [26,27]. Very large grain size reduced the coercive field increases. The remanent polarization reflects the internal polarizability of the material. Therefore, high is the remanent polarization, high is the polarizability of the material.

The values obtained for the remaining polarization ( $P_r$ ) and the coercitive field ( $E_c$ ) are in accordance with the results obtained by the SEM characterization.

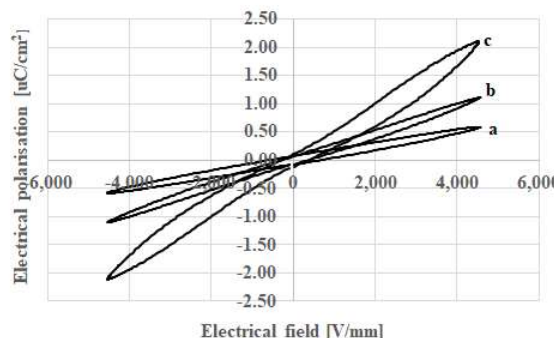


**Fig. 9** - Room temperature ferroelectric hysteresis loops of sintered compositions la 1100°C/ 2 h: (a) PZTF-42, (b) PZTF-52 and (c) PZTF-58/ *Curbele de histerezis la temperatura camerei ale compozițiilor sinterizate la 1100°C/ 2 h: (a) PZTF-42, (b) PZTF-52 și (c) PZTF-58.*

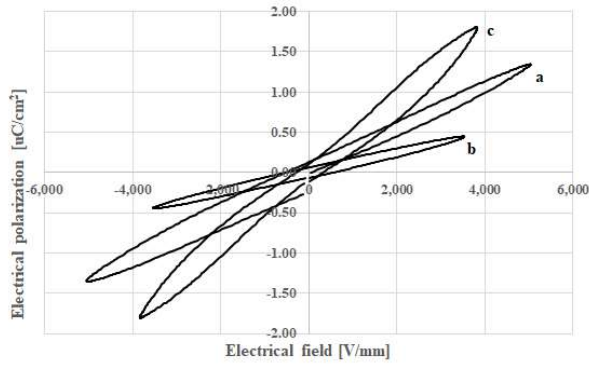


**Fig. 10** - Room temperature ferroelectric hysteresis loops of sintered compositions la 1150°C/ 2h: (a) PZTF-42, (b) PZTF-52 and (c) PZTF-58/ *Curbele de histeresis la temperatura camerei ale compozițiilor sinterizate la 1150°C/ 2 h: (a) PZTF-42, (b) PZTF-52 și (c) PZTF-58.*

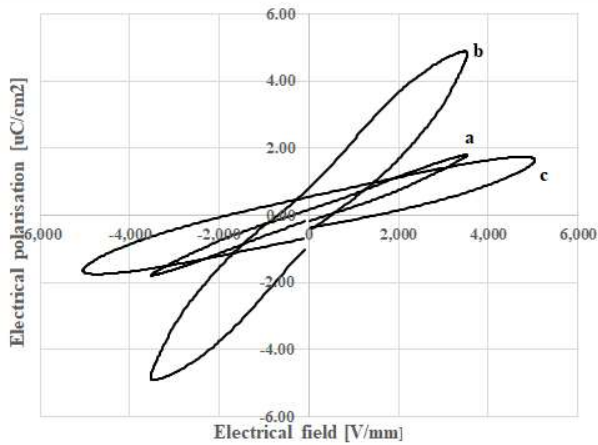


**Fig. 11** - Room temperature ferroelectric hysteresis loops of sintered compositions (1200°C/ 2h): (a) PZTF-42, (b) PZTF-52 and (c) PZTF-58/ *Curbele de histeresis la temperatura camerei ale compozițiilor sinterizate la 1200°C/ 2 h: (a) PZTF-42, (b) PZTF-52 și (c) PZTF-58.*

**3.5. Dielectric and Piezoelectric properties**

At high sintering temperature, because of the decreasing of the number of pores, the dielectric and piezoelectric properties increase considerably associated to domain walls mobility.

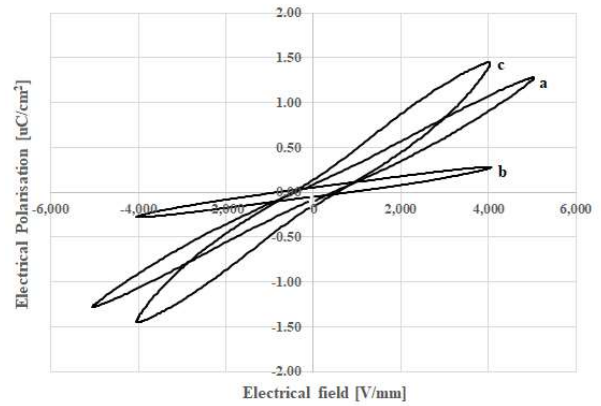


**Fig. 12** - Room temperature ferroelectric hysteresis loops of sintered compositions (1250°C/ 2h): (a) PZTF-42,(b) PZTF-52 and (c) PZTF-58/ *Curbele de histeresis la temperatura camerei ale compozițiilor sinterizate la 1250°C/ 2 h: (a) PZTF-42,(b) PZTF-52 și (c) PZTF-58.*

Table 2 reports the obtained values for the dielectric (loss factor (tan δ) at 1 kHz, relative dielectric constant (ε<sub>r</sub>) at room temperature, Curie temperature (T<sub>c</sub>) and resistivity (R<sub>v</sub>)) and piezoelectric properties (the planar electromechanical factor k<sub>p</sub> and the transversal electromechanical factor k<sub>t</sub>) of the compositions PZTF-42, PZTF-52 and PZTF-58 sintered at 1250°C for 2h. The anisotropy has been determined by the ratio k<sub>t</sub>/k<sub>p</sub>.

To determine the Curie transition temperature, the dielectric constant has been measured as a function of temperature at 1 kHz. The compositions show a typical ferroelectric phase transition peak at a Curie transition temperature higher than 445 °C. It can be observed that all the values depend on the Zr<sup>4+</sup>/Ti<sup>4+</sup> ratio.

The anisotropy of poled compositions sintered at 1250°C is higher than 10, indicating a superior grade of alignment of the domains during poling. Densification and homogeneity of the ceramics are still the main factors of the improved piezoelectric properties.

**Table 2**

The dielectric and piezoelectric properties for the all compositions sintered at 1250°C for 2h/ *Proprietățile dielectrice și piezoelectrice pentru toate compozițiile sinterizate la 1250°C timp de 2h*

Compositions	tan δ	ε <sub>r</sub>	R <sub>v</sub> *10 <sup>17</sup> (Ω*cm)	T <sub>c</sub> [°C]	k <sub>p</sub>	k <sub>t</sub>	k <sub>t</sub> /k <sub>p</sub>
PZTF-42	0.0044	394	20.4	>445	0.42	7.57	18.02
PZTF-52	0.0018	253	11.7	>445	0.44	7.57	17.20
PZTF-58	0.0130	464	6.5	>445	0.42	7.57	18.02

At 1100°C and 1150°C, the compositions could not be polarized. The structural inhomogeneity being the determining factor in this process. For the compositions sintered at the highest temperatures (1200°C and 1250°C) some results have been reported in a previous research paper [28].

**4. Conclusions**

In the present research paper, the ferroelectric compositions described by the general formula Pb(Zr<sub>λ</sub>Ti<sub>1-λ</sub>)<sub>1-3x/4</sub>Fe<sub>x</sub>O<sub>3</sub> were synthesized by solid state reaction using high temperature; the obtained materials were investigated with the aim to

determine if there is the possibility to employ them as sputtering target during deposition technology. The dopant ( $Fe^{3+}$ ) was diffused onto the PZT lattice and all the sintered ferroelectric compositions revealed a good homogeneity. The results obtained indicate an influence of the  $Zr^{4+}/Ti^{4+}$  ratio on the dielectric and piezoelectric properties of the analysed compositions. The evolution of the grains size is directly associated to the sintering temperature and to the  $Zr^{4+}/Ti^{4+}$  ratio. As dielectric and piezoelectric properties concern, it was observed that all the compositions sintered at 1100°C and 1150°C could not be polarized because of their structural inhomogeneity.

For the reason that usually targets to be used in deposition procedures are sintered at high temperatures, the research was carried out using temperatures which lead to achieve a denser, more compact and homogeneous ceramic structure which can be easily pull-out during the deposition procedure. In fact, the best results, in terms of in terms of the  $Fe^{3+}$  doped PZT materials structure, were achieved at the highest sintering temperature: such material obtained exhibits some challenging features, i.e. the effects coming from the presence of high anisotropy piezo-active elements, revealing that they can be considered as a promising material to be properly exploited as target in sputtering techniques, leading in-house production saving time and capital.

**Acknowledgements**

The authors acknowledge the financial support of the Ministry of Research and Innovation, through PN 19310103/ 2019 and from Subsidiary contract type D, no.133-D1 ICPE "Rotary system of positioning with piezoelectric motor".

**REFERENCES**

[1] B. Jaffe, W.R. Cook, H. Jaffe, Piezoelectric Ceramics, Academic Press, London and New York, 1971, 317

[2] S. L. Swartz, Topics in electronic ceramics. IEEE Transactions on Electrical Insulation, 1990, **25(5)**, 935–987

[3] V. A. Isupov, Comments on the paper "X-ray study of the PZT solid solutions near the morphotropic phase transition." Solid State Communications, 1975, **17(11)**, 1331–1333

[4] V. A. Isupov, Phase coexistence in lead zirconate titanate solid solutions, Physics of the Solid State, 2001, **43(12)**, 2262–2266

[5] P. Ari-Gur, și L. Benguigui, X-ray study of the PZT solid solutions near the morphotropic phase transition. Solid State Communications, 1974, **15(6)**, 1077–1079

[6] M. Morozov, "Softening and hardening transitions in ferroelectric Pb(Zr,Ti)O<sub>3</sub> ceramics," Ph.D. dissertation, Ecole Polytechnique Fédérale de Lausanne, 2005

[7] K. Kakegawa, J. Mohri, T. Takahashi, H. Yamamura și S. Shirasaki, A compositional fluctuation and properties of Pb(Zr, Ti)O<sub>3</sub>. Solid State Communications, 1977, **24(11)**, 769–772

[8] D. Dal-Hyun, "Investigation of ferroelectricity and piezoelectricity in ferroelectric thin film capacitors using synchrotron x-ray microdiffraction", A dissertation submitted in partial fulfillment of the requirements for the degree of Doctor of Philosophy (Metallurgical Engineering) at the UNIVERSITY OF WISCONSIN-MADISON, 2006

[9] J. Qi și H. Ji, Research on applications of piezoelectric materials in smart structures, Frontiers of Mechanical Engineering in China, 2011, **6**, 99–111

[10] B. Noheda, D. E. Cox, G. Shirane, J. A. Gonzalo, L. E. Cross și S.-E. Park, A monoclinic ferroelectric phase in the Pb(Zr<sub>1-x</sub>Ti<sub>x</sub>)O<sub>3</sub> solid solution, Applied Physics Letters, 1999, **74(14)**, 2059–2061

[11] B. Noheda, D. E. Cox, G. Shirane R. Guo, B. Jones, L. E. Cross, Stability of the monoclinic phase in the ferroelectric perovskite PbZr<sub>1-x</sub>Ti<sub>x</sub>O<sub>3</sub>, Physical Review B, 2000, **63(1)**

[12] G. H. Haertling, Ferroelectric Ceramics: History and Technology, Journal of the American Ceramic Society, 1999, **82(4)**, 797–818

[13] S. A. Wilson, R. P. Jourdain, J. Zhang, Q. Dorey, R. A. Bowen, C. R. Willander, M. K Persson, New materials for micro-scale sensors and actuators. Materials Science and Engineering: R: Reports, 2007, **56(1-6)**, 1–129

[14] Turik A.V., Topolov, V.Yu., Ferroelectric ceramics with a large piezoelectric anisotropy, Journal of Applied Physics, 1997, **30**, 1541-1549

[15] X. Yao, Z. L. Yin, L. E. Cross, Polarization and depolarization behavior of hot pressed lead lanthanum zirconate titanate ceramics, Journal of Applied Physics, 1983, **54**, 3399-3403

[16] M. I. Morozov, D. Damjanovic, Charge migration in Pb(Zr,Ti)O<sub>3</sub> ceramics and its relation to ageing, hardening, and softening, Journal of Applied Physics, 2010, **107**, 034106-1- 034106-9

[17] C. Miclea, C. Tanasoiu, C. F. Miclea, , L. Amarande, , A. Gheorghiu, F. N. Sima, Effect of iron and nickel substitution on the piezoelectric properties of PZT type ceramics, Journal of the European Ceramic Society, 2005, **25(12)**, 2397–2400

[18] C. Moure, M. Villegas, J. F. Fernández, P. Durán, Microstructural and piezoelectric properties of fine grained PZT ceramics doped with donor and/or acceptor cations, Ferroelectrics, 1992, **127(1)**, 113–118

[19] R. Rai, S. Mishra, N. K. Singh, Effect of Fe and Mn doping at B-site of PLZT ceramics on dielectric properties, Journal of Alloys and Compounds, 2009, **487(1-2)**, 494–498

[20] J. E. Garcia, R. Pérez, A. Albareda, J. A. Eiras, Non-linear dielectric and piezoelectric response in undoped and Nb<sup>5+</sup> or Fe<sup>3+</sup> doped PZT ceramic system, Journal of the European Ceramic Society, 2007, **27(13-15)**, 4029–4032

[21] D. Wang, H. Guo, C. S. Morandi, C. A. Randall, , S. Trolrier-McKinstry, Cold sintering and electrical characterization of lead zirconate titanate piezoelectric ceramics, APL Materials, 2018, **6(1)**, 016101, 016101-1-016101-7

[22] F. Kahoul, L. Hamzioui, A. Boutarfaia, The Influence of Zr/Ti Content on the Morphotropic Phase Boundary and on the Properties of PZT-SFN Piezoelectric Ceramics. Energy Procedia, 2014, **50**, .87–96

[23] K. Carl, K. H. Hardtl, Electrical after-effects in Pb(Ti, Zr)O<sub>3</sub> ceramics, Ferroelectrics, 1977, **17(1)**, 473–486

[24] T. M. Kamel, G de With., Poling of hard ferroelectric PZT ceramics, Journal of the European Ceramic Society, 2008, **28(9)**, 1827–1838

[25] M. Morozov, D. Damjanovic, N. Setter, The nonlinearity and subswitching hysteresis in hard and soft PZT, Journal of the European Ceramic Society, 2005, **25(12)**, 2483–2486

[26] W. L. Warren, G. E. Pike, K. Vanheusden, D. Dimos, B. A. Tuttle, J. Robertson, Defect-dipole alignment and tetragonal strain in ferroelectrics, Journal of Applied Physics, 1996, **79(12)**, 9250–9257

[27] W. L. Warren, K. Vanheusden, , D. Pike Dimos, Tuttle G. E., B. A., Oxygen Vacancy Motion in Perovskite Oxides. Journal of the American Ceramic Society, 1996, **79(2)**, 536–538

[28] A.I. Dumitru, F. Clicinschi, T.G. Dumitru, D. Pătroi, J. Pinte, G. Velciu, I Peter., Effects of Sintering Temperature on Structural and Electrical Properties of Iron Doping PZT Ceramics, Acta Marisiensis. Seria Technologica, 2020, **18(2)**, 105-114

\*\*\*\*\*